



1 **Soil salinization risk assessment owing to poor water quality drip**
2 **irrigation: A case study from an olive plantation at the arid to semi-arid**
3 **Beit She'an Valley, Israel**

4 **Vladimir Mirlas¹, Yaakov Anker^{1*}, Asher Aizenkod² and Naftali Goldshleger¹**

5 1- The department of chemical engineering and The Eastern R&D center, Ariel University,
6 Israel

7 2- The Plant Protection and Inspection Services of the Ministry of Agriculture and Rural
8 Development, Israel

9 *- Corresponding author: Yaakov Anker (kobia@ariel.ac.il)

10 **Abstract**

11 Salinization causes soil degradation and soil fertility reduction. The main reasons for
12 soil salinization are poor irrigation water quality and incorrect irrigation management.
13 Soil salinization is accelerated owing to irrigation with treated wastewater with
14 elevated salt concentration. The study area is located in the Beit She'an Valley, one of
15 the most important agricultural regions in Israel. The combination of soil salinization
16 and poor drainage conditions impedes plant development and is manifested in
17 economic damage to crops. Without clear irrigation criteria, an increase in soil salinity
18 and steady damage to soil fertility might occur. The study objective was to provide an
19 assessment of soil salting processes as a result of low-quality irrigation water at the
20 Kibbutz Meirav olive plantation. This study combined various research methods,
21 including soil salinity monitoring, field experiments, remote sensing (FDEM), and
22 unsaturated soil profile saline water movement modeling. The assessment included the
23 salinization processes of chalky soil under drip irrigation by water with various
24 qualities. With a drip irrigation regime of water with a dissolved salt content of 3.13
25 dS/m, the salinization process is characterized by salts accumulation in the upper root
26 zone of the trees. The modeling results showed that there is a soil salinization danger
27 in using brackish water and that irrigation with potable water helps to reduce soil
28 salinization.

29

30 **Keywords: Soil Salinity; Irrigation; Remote sensing; Soil salinization mapping;**
31 **Modeling**

32

33



34 **1. Introduction**

35 Soil salinity surveys and studies across the world and, in particular, in Israel indicate
36 that irrigation with poor water quality and improper irrigation management causes soil
37 salinization and degradation, and also damages soil fertility (Wada et al., 2016; Pandit
38 et al., 2020). Soil salinity monitoring in the Jezre'el Valley began in 1987, following a
39 soil salinity survey that showed intensive salinization and often alkalization of the
40 upper soil horizons (Benjaminy et al., 2005, 1998, 2000). Earlier studies (Gafni et al.,
41 1990) had shown that these processes were enhanced by a semi-confined shallow
42 aquifer (Kruseman and De Ridder, 1976), causing upward water flow during winter
43 and spring seasons and reducing downward rain and irrigation percolation during the
44 summer and fall seasons.

45 Most of the soil salinization problems in the Beit She'an Valley are affiliated with the
46 use of poor-quality irrigation water. The soil salinity is constantly increasing, owing to
47 irrigation with high salinity-treated wastewater and blocking of the natural drainage to
48 the underlying groundwater (Mirlas et al., 2006; Mirlas, 2012). At a lemon tree
49 plantation in the Jordan Valley, it was found that an increase in irrigation water
50 salinity to 3.7 times freshwater salinity, increased soil salinity by 3.8-4.1 times during
51 few years (Abu Awwad, 2001). Additional effects of treated effluent irrigation in the
52 Jordan Valley were pH decrease in parallel to soil salinity increase (Mohammad and
53 Mazahreh, 2003). High saline-sodic concentration in irrigation damaged the soil's
54 hydraulic conductivity, increasing runoff and silt-clay chalk soil erosion in the Beit
55 She'an Valley (Mandal et al., 2008a; Bhardwaj et al., 2008).

56 While global scale land surface-soil-biosphere-atmosphere models enables a regional
57 water balance (Boone et al., 2017; Guimberteau et al., 2018), understanding water and
58 solute movement processes in unsaturated soil layers requires a mathematical
59 description and numerical model development (Leij et al., 1991; Simunek and van
60 Genuchten, 1995; van Genuchten and Wagenet, 1989, Celia et al., 1990; Kool et al.,
61 1985). Using principal component analysis (PCA), it was found that soil hydraulic
62 conductivity is one of the important factors affecting soil quality (Mandal et al.,
63 2008b). Water and solute movement models in an unsaturated soil layer are based on
64 Richards' equation for one-dimensional movement of water under saturation variability



65 (Celia et al., 1990; Bear, 1972) and root water uptake is calculated by the van
66 Genuchten equation (van Genuchten, 1987). In such models, the soil hydraulic
67 conductivity coefficient in the saturated media varies as a function of the soil's
68 hydraulic conductivity.

69 Soil moisture may be evaluated through atmospheric conditions (Garrigues et al.,
70 2015), or calculated as a function of suction (pressure head) and hydraulic
71 conductivity in an unsaturated condition. Salt leaching and accumulation is significant
72 in arid and semi-arid areas (Wada et al., 2016). Models of salt motion are commonly
73 based on the Fickian convection-dispersion equation for solute transport (Toride et al.,
74 1993) and complex models should also consider absorption processes, anion and
75 cation exchange, and more. Several modeling platforms such as "HYDRUS"
76 (Simunek et al., 1998) and "WASTRC-1" (Mirlas et al., 2006) are widely used. The
77 WASTRC-1, one-dimensional water and solute movement model of under saturated
78 conditions, was found to fit the soil characteristics of Hula Valley irrigated fields in
79 Israel. In both "HYDRUS" and "WASTRC-1" models, various soil hydraulic
80 conditions such as drainage, irrigation, layer saturation depth can be considered. Soil
81 density, saturated hydraulic conductivity, field moisture, suction, and root zone
82 development among other factors are prerequisites for model calibration, parameter
83 validation, and, consequently, proper water and solute movement simulation
84 (Garrigues et al., 2015).

85 Salinization during irrigation is a dynamic process as the number of salts in the soil
86 and their composition change during irrigation both in the area and in the soil profile.
87 Soil salinity mapping by the traditional sampling method is expensive and time-
88 consuming, with mapping accuracy directly depending on the distance between the
89 sampling points. Remote sensing technologies that are based on active electromagnetic
90 (EM) radiation are being widely adopted for soil salinity mapping. Ground-based EM
91 methods measure electrical conductivity (EC) in subsurface and substratum horizons
92 and can thus recognize salinity anomalies in the field before salinization approaches
93 the surface (Farifteh et al., 2007). EM induction sensors measure the soil profile
94 salinity by recording the soil's apparent electrical conductivity (ECa).



95 Frequency-domain electromagnetic techniques (FDEM) are a powerful tool for
96 mapping soils and detecting changes in soil types related to salinity. FDEM sensors
97 work within a range of 30 cm to 5 m depth and perform best while scanning the area
98 from about 1m above the ground (Ben Dor et al., 2009a). By applying FDEM with
99 other active and passive remote sensing methods, EC values in given soil layers were
100 attained for the soil in Jezre'el Valley (Ben Dor et al., 2009b).

101 The soils of the Beit She'an Valley were selected for research as it is one of the most
102 important agricultural areas in Israel. They consist of brown clay soils (gumusols) and
103 chalky soils, with the latter's profile characterized by thin layers and formation layers
104 of marl with high water absorption capacity. The soil stratification influences the
105 potential to drain and wash excess salts that accumulate during the irrigation season,
106 which preserve ventilated root conditions. Sodium rich soil has up to 30% cation
107 exchangeable capacity, which exacerbates the ventilation conditions necessary for
108 plants. The combination of soil stratification and poor drainage conditions impedes
109 plant development and, in some cases, the soil structure destruction and salts
110 accumulation in the root zone causes plant degeneration due to water absorption
111 difficulties (Machado and Serralheiro, 2017). As a consequence, crop irrigation by
112 brackish water in the Beit She'an area might cause economic damage.

113 The irrigation water sources in the area are of variable quality: springs and Jordan
114 River water are considered of acceptable quality, while groundwater and also effluent
115 water might be of poor quality. In this latter case, low irrigation water quality without
116 clear irrigation criteria might steadily damage soil fertility. Defining an irrigation
117 regime for local soil and water quality conditions is, therefore, of great importance for
118 preventing crop and economic damage in the Beit She'an Valley. This knowledge can
119 indicate how water and salt move in soil and correlate to salinity processes and
120 irrigation management capability. Combining remote sensing (FDEM) methods with
121 water and salt movement models in the unsaturated soil layer may enable effective
122 identification of soil salting processes. In turn, this may result in improved planning
123 and control of irrigation systems.



124 As an integrative knowledge harvesting demonstration needed for irrigation
125 management, this study's objective was to assess soil salting processes as a result of
126 low-quality irrigation at the Kibbutz Meirav olive plantation in the Beit She'an Valley.

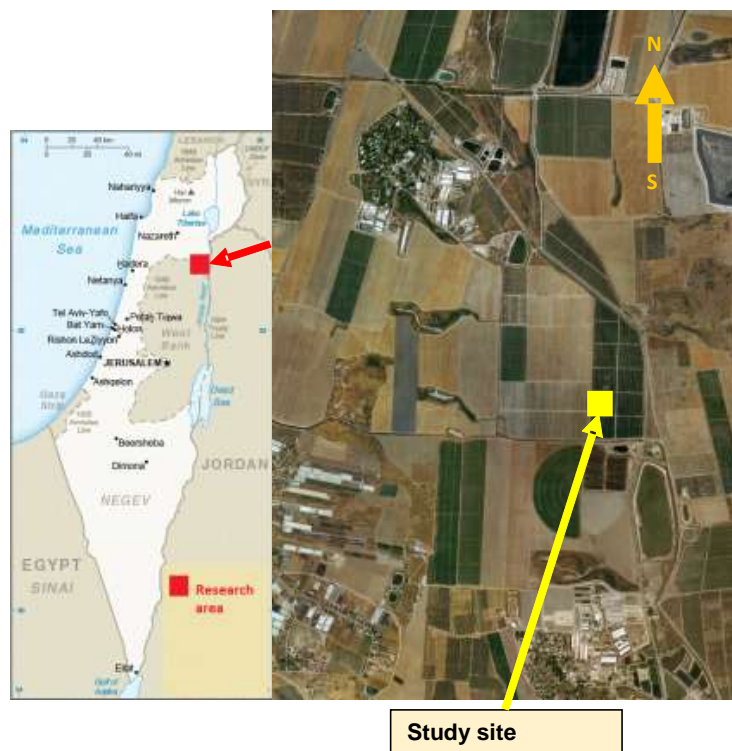
127

128 2. Materials and Methods

129

130 2.1. Research Site background and geographical framework

131 The Beit She'an area is a unique agricultural area due to a combination of warm and
132 dry climate (annual evaporation of 2400 mm at the meteorological service, Eden Farm
133 Station), saline water irrigation, and heavy soils. The study site is Kibbutz Meirav, a
134 mature (2002) olive plantation located 1100 m north of the Kibbutz (Fig.1.).



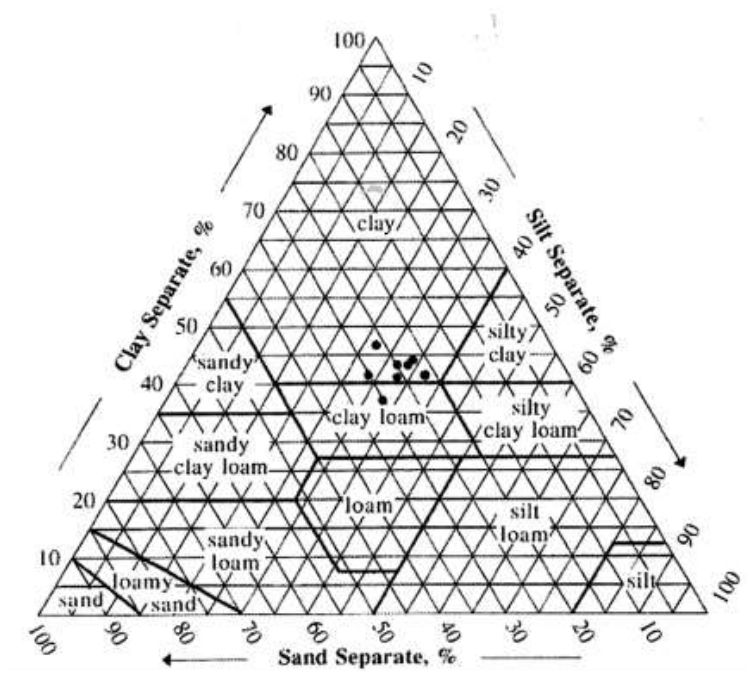
135

136 Fig. 1. Study site location (regional map: after CIA factbook)

137



138 The planting intervals between the trees rows are 7 m and 4 m. The rainfall amount in
139 the study site was 154, 253 and 281mm in 2007/8, 2008/9, and 2009/10 hydrological
140 years, respectively. The soil in the study site is layered, with a practically impervious
141 shallow layer of travertine found in different locations of the plantation as well as
142 layers of marl at greater depth. Soil salinity stains were observed together with trees
143 suffering from lack of ventilation, salting and excess irrigated water. Following the
144 results of soil sample particle size analysis, the mechanical components of the soil at
145 the research site consist of clay (40-50%), silt (25-30%) and sand (20-30%) (Fig.2.).



146
147 Fig. 2. The mechanical composition (Soil texture triangle) of soil at the research site.
148 The depth of the travertine layer range is from 110 cm at the southern edge to 55-60
149 cm at the northern edge of the site (Fig. 3).



150

151 Fig. 3. Depth of travertine layer from the soil surface, cm

152 1- lithological borehole; 2- isoline of travertine layer depth from the soil surface

153

154 The main irrigation water sources in the area are Jordan River water and local
 155 groundwater whose salinity and SAR ratio are very high, mainly due to high sodium
 156 chloride concentrations. The chloride concentration is at a range of 800 - 1700 mg/l
 157 and electrical conductivity is above 3.5 dS/m. Local authorities intend to dilute the
 158 local water by effluent water and reduce the chloride concentration in water to 800
 159 mg/l.

160 The Kibbutz Meirav olive plantation irrigation water quality test results for different
 161 seasons during the study period are presented in Table 1.

162

163 Table 1. Quality of irrigation water in Kibbutz Meirav olive plantation

164

B ppm	N-NH4 mg/l	N-NO3 mg/l	SAR	Cl ppm	Ca+Mg meq/l	Na meq/l	K meq/l	EC dS/m	pH	Date
0.139			5.1	862	14	13.5	0.36	2.9	7.9	13.06.10
			6.4	1004.7	16.7	18.5	0.45	3.74	8.2	22.08.10
			5.21	844.9	16.6	15	0.32	3.19	8.1	19.12.10
0.11	1.9	N.D.	5.71	841.4	13.6	15	0.31	2.84	8.9	5.05.11
0.2	0.8	N.D.	5.66	848	14.6	15.3	0.42	3.64	8.2	23.08.11

165

166

167

168



169 The olive plantation drip irrigation regime in one extension along the row that was
170 used for the study calibration was daily 1 l/s every 40 cm, with cumulative water
171 amount from April to November (harvest) of between 631 to 1272 cubic meters per
172 dunam. Nitrogen fertilizer given by dosing pumps was 15 - 20 kg for the season
173 regardless of the amount of water.

174

175 **2.2. Research methodology**

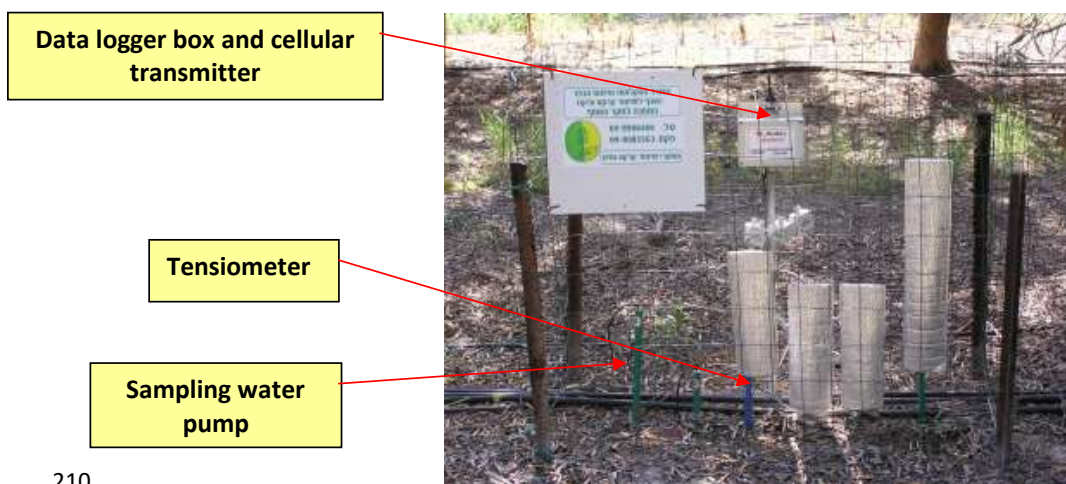
176

177 This study integrates field experiments with water and salt movement models in the
178 unsaturated soil strata. Field experiments including remote sensing method (FDEM)
179 were utilized to supply the required data for water and salt movement modeling and
180 soil salinity mapping during soil salinization monitoring under different irrigation
181 conditions (Corwin and Lesch, 2005). The suction and soil moisture monitoring during
182 the irrigation period was conducted near two tensiometer stations characterizing
183 suction and soil moisture conditions. The first station characterized irrigation by about
184 80% of normal irrigation (lack of water) and the second station characterized irrigation
185 by about 120% of normal irrigation (excess water). The field experiment was
186 conducted in spring before beginning summer irrigation, which made it possible to
187 evaluate the soil salinization dynamics when water enters practically dry soil after
188 winter precipitation salt washing. The experiment included soil sampling to measure
189 soil moisture and soil salinity that was coupled to FDEM mapping. The integration of
190 the various data processing types and modeling finally yielded a soil salinization
191 spatial-temporal illustration of the different irrigation regimes (Fig. 4).

192



207 view data "on-line". During the study, selected soil solution samples were pumped
208 from the tensiometers and analyzed at the lab (Fig.5.).
209



210
211

212 Fig. 5. Transmitting tensiometer station.

213

214 *Soil salinity and moisture monitoring*

215 Soil moisture and salinity monitoring were made by simultaneous soil sampling every
216 two weeks from September until December 2011. Soil samples were taken at depths of
217 0-20, 40-60, 20-40 and 70 cm or down to the depth of the travertine layer. Drilling was
218 done along the olive rows between the trees. Each sample characterized a particular
219 tensiometer depth as well as distance from the irrigation pipe and closest dripper. The
220 laboratory salt composition delineation included: electrical conductivity (EC),
221 saturation percentage (SP), sodium adsorption ratio (SAR), Na, Ca + Mg, Cl, SO₄ ion
222 concentrations, general chalk, mechanical composition, and soil moisture.

223

224 *Field experiment.*

225 On 22-28.03.2011, a field experiment was conducted, with the purpose to obtain soil
226 salinity parameters before the irrigation season. These parameters were needed to build
227 and adapt the moisture and salts motion model for the upper soil unsaturated layer.
228 The experiment included moisture and salinity measurements through manual soil



229 sampling and FDEM soil salinity mapping. Near each tensiometer station, three
230 control lines were marked perpendicular to the dripper line, whereas the line center
231 was positioned near the dripper. Near the first tensiometer station, the distance
232 between the control lines (1A, 1B, 1C) was 50 cm and near the second tensiometer
233 station (2A, 2B, 2C) it was 40 cm (according to distance changes between the drippers
234 so that each control line was extended from the middle between the three rows). Soil
235 sampled for laboratory salt composition and moisture tests were taken for each control
236 line, at a central point adjacent to the dripper and 30,80,180 and 330 cm distances
237 from the central sampling point on both sides. Together with soil sampling, values of
238 soil suction from the tensiometers were also measured. The first soil sampling was
239 done at 08:30 am before irrigation on control lines 1A and 2A. At 09:00, drip
240 irrigation began with an intensity of 1.6 liters per hour and stopped at 10:15. At 12:15
241 immediately after the irrigation finished (2 hours after irrigation commences),
242 sampling was done on lines 1B and 2B soil at the central point and 30 cm distance
243 from it on both sides. On March 23 and March 24, a total of 30 mm of rain fell, which
244 was recorded by the automatic monitoring.

245

246 *Measurements and mapping of soil electrical conductivity using FDEM*

247

248 FDEM measurements were carried out along the control lines and in the area between
249 the tree row in the experiment site. Three measuring lines with 7 m length were spaced
250 0.5 m apart near the first tensiometer station. The measurement lines were made
251 perpendicular to the irrigation dripper pipeline. Mapping was done after three hours of
252 irrigation. Five channels with different frequency: 62525; 22075; 7825; 2275; and 975
253 Hz were used for characterizing intervals of soil layer depth: 0-30 cm; 0-45 cm; 0-60
254 cm; 0-75 cm; and 0-100 cm, respectively. Interpolation and spatial soil salinity
255 mapping (in EC, dS/m) were performed using SURFER software.

256

257

258 *Water and salt movement mode development and application for soil salinization*
259 *assessment and prediction.*



260 The water and salt movement model in the upper unsaturated soil layer and up to the
261 travertine layer was made in the HYDRUS 1D software. The one-dimensional model
262 characterizes the cross-section to a depth of 60 cm above the travertine layer.

263 The water and salt movement, a basic mathematical model of one-dimensional
264 equations for an unsaturated soil state, was:

$$265 \quad \partial W / \partial t = \partial / \partial x [K(W) (\partial H / \partial x)] - E(W, x) \quad (1)$$

$$266 \quad K(W) = f(K_s, W) \quad (2)$$

$$267 \quad \partial WC / \partial t = \partial / \partial x [D^* (\partial C / \partial x)] - \partial VC / \partial x - S(C) \quad (3)$$

268 where:

269 W - Volumetric Moisture

270 H - Suction

271 K (W) - Hydraulic conductivity of unsaturated soil state

272 E - Plant root moisture absorption function

273 K_s - Hydraulic conductivity of soil in a saturated state

274 C - Soil solution salts concentration

275 D* - Soil salts diffusion coefficient

276 S - Soil salt absorbing (or releasing) function as a result of moisture changes

277 t - Time

278 The hydraulic model used was the van Genuchten-Mualem (no hysteresis) single
279 porosity model (van Genuchten, 1980). As a soil salinization model, Crank-Nicholson
280 was used as a time weighting scheme (Crank and Nicolson, 1947) and the Galerkin
281 Finite Scheme (Fletcher, 1983) for a space weighting scheme equilibrium model. For
282 water movement relation with the root zone, the Feddes water uptake reduction model
283 (Feddes et al., 2001) was used, with maximum concentration to passive root solute
284 uptake of 0.5 (cRoot). The one-dimensional model calculated the volumetric moisture
285 and total salinity in a soil profile down to the model's lower boundary. In the
286 HYDRUS 1D software, the unsaturated layer parameters are automatically determined
287 by the soil type. The lower boundary of the water movement model was calculated as
288 a constant flow along the travertine layer.

289 The irrigation input to the soil profile through the model's upper boundary was
290 calculated as the water supply according to the momentary irrigation regime.



291 Evapotranspiration and transpiration values and also root zone activity was determined
292 from the field data and changed during the irrigation season. The models were
293 calibrated according to the field experiment data. The calibrated model was used to
294 assess and predict soil salinization due to irrigation with different water quality: 3.13
295 dS/m (available today); 1.5 dS/m (potable water); and 5.5 dS/m (brackish water). The
296 time step of the model was a month and the salinity and moisture distribution during
297 this month was used as the initial conditions for the following month.

298

299 **3. Results and Discussion**

300

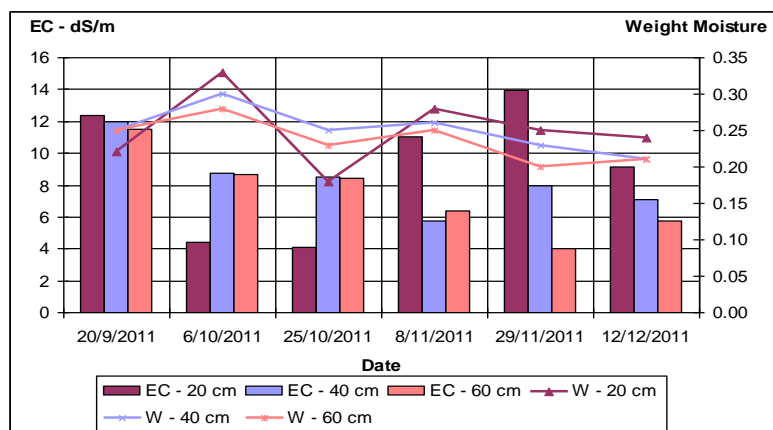
301 ***3.1. Soil moisture and salinization dynamics in the autumn, following the*** 302 ***intensive summer irrigation.***

303

304 Near the first tensiometer station at a depth of about 60 cm of the travertine layer and
305 irrigation by about 80% of normal (lack of water), the soil salinity was about 11-12
306 dS/m in the soil profile in September (Fig. 6). After the last takt of irrigation at the
307 beginning of October, the soil salinity decreased to 4-8 dS/m throughout the soil
308 profile and especially in the top layer. Soil weight moisture increased from 0.22-0.25
309 to 0.33 at the top of the soil profile. Then, before the rainfall in mid-December, soil
310 salinization gradually increased, and the most intense salinization growth to 14 dS/m
311 was found in the upper layer (0-20 cm) of soil. The weight moisture values gradually
312 decreased to 0.2-0.25, whilst the highest values were noted in the upper layer of the
313 soil profile.

314 Near the second tensiometer station with a travertine layer depth of about 70 cm and
315 irrigation by about 120% of normal (excess water), soil salinity was lower, between
316 2.0 to 4.0 dS/m. In the upper layer (0-20 cm), soil salinity exceeded 6 dS/m and after
317 the last takt of irrigation at the beginning of October, it increased to 14 dS/m with
318 gradual decrease to previous values during November-December. The moisture weight
319 values were almost the same throughout the soil profile, and gradually decreased from
320 0.35 to 0.2 during the monitoring period.

321



322

323

324

325

Fig. 6. Changes in soil salinity (EC) and soil weight moisture (W) during the autumn near the first tensiometer station.

326

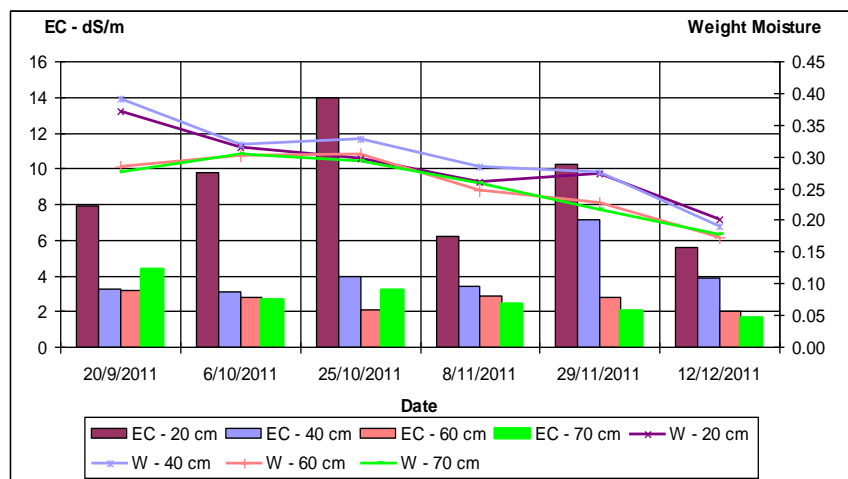
327

328

329

330

The SAR values under irrigation conditions of about 80% of normal ranged from 4 to 12. The SAR values increased with soil profile depth. Under irrigation conditions of about 120% of normal (excess water), SAR values were found to be lower, ranging from 3 to 6, with an increase toward the upper soil layer.



331

332

333

334

Fig. 7. Changes in soil salinity (EC) and soil weight moisture (W) during the autumn near the second tensiometer station.



335 Near the first tensiometer station with a depth of about 60 cm of the travertine layer
336 and irrigation by about 80% of normal (lack of water) at the end of September, the
337 chloride concentration was high throughout the soil profile and ranged from 3200 to
338 3500 mg per liter. At the end of the irrigation period, the chloride concentration again
339 increased to a range of 3500-4000 mg per liter in the upper layer (20 cm). After the
340 last takt of irrigation at the beginning of October, the chloride concentration decreased
341 to 1000 mg per liter in the upper layer (20 cm). After the end of irrigation, the chloride
342 concentration again increased to a range of 3500-4000 mg per liter in this layer. The
343 sulfate concentration hardly changed and ranged from 300 to 550 mg per liter
344 throughout the soil profile.

345 Near the second tensiometer station with a travertine layer at a depth of about 70 cm
346 and irrigation of about 120% of normal (excess water), chloride concentrations were
347 found to be lower, ranging from 400 to 3000 mg per liter during the study period. The
348 chloride concentration increased during irrigation and decreased at the end of
349 irrigation in the deeper soil layers. No clear relationship was found between the
350 chloride concentration and the soil moisture. The sulfate concentration ranged from
351 100 to 600 mg per liter throughout the soil profile.

352 The amount of general chalk in the soil was very high and hardly changed during the
353 study period. The amount of general chalk ranged from 70% to 85% and did not
354 depend on soil moisture and irrigation regime.

355

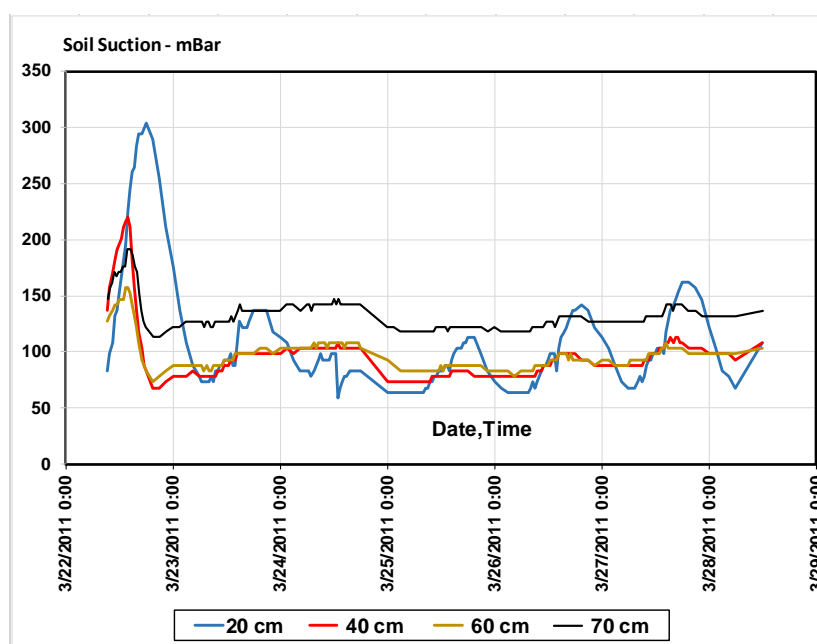
356 ***3.2. Assessment of drip irrigation effect on soil salinization.***

357

358 The soil suction that was measured in-situ using the first tensiometer station is shown
359 in Figure 8. In station 1, the soil suction before irrigation varied from 140 to 300 mbar
360 depending on the depth of the measured soil layer, while after irrigation it dropped to
361 40-130 mbar. Due to the highest moisture, the maximal soil suction decrease was
362 observed in the upper soil layer (0-20 cm). While in the upper soil layer (0-20 cm)
363 sinusoidal oscillations were observed due to daily (day-night) changes in temperature
364 and humidity. At other depths, once settled the suction had a small tendency to
365 increase during the study period.



366



367

368

369 Fig. 8. Soil suction on the different depth of soil profile, measured at the first
370 tensiometer station.

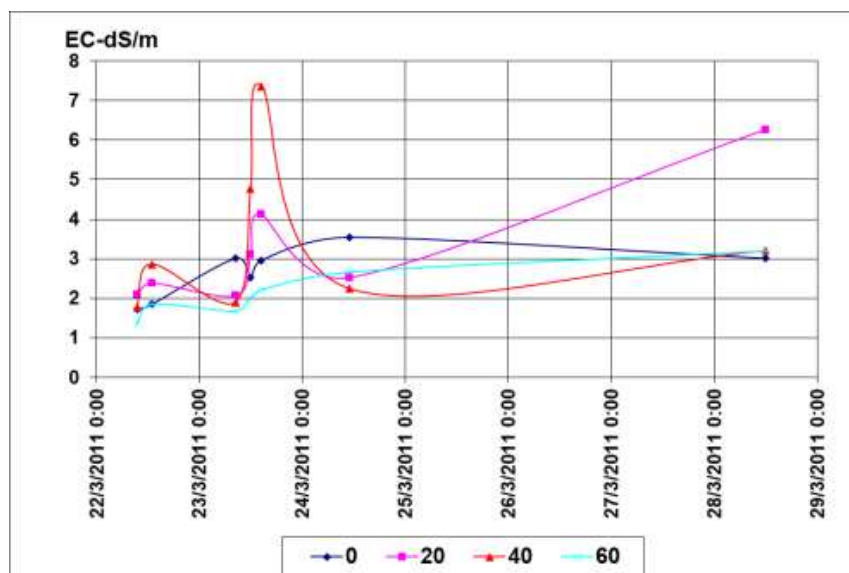
371

372 Laboratory soil salinity measurements characterized the dissolved salt concentration in
373 the soil saturated solution near the drippers. Soil salinity near the first tensiometer
374 station ranged from 1.5 dS/m before irrigation to 7.5 dS/m after 22 hours from when
375 irrigation commenced. Salinity differences by depth are irregular, but the rain event on
376 23/3/2011 was noticed at 40 cm and the increase of 20 cm during the following days
377 may indicate capillary movement (Fig. 9).

378 The highest soil salinity from 4.1 to 7.4 dS/m was detected at depths of 20-40 cm. The
379 presence of a salinization peak in the soil layer at a depth of up to 40 cm was
380 associated with the leaching of salts to a depth with irrigation water. The subsequent
381 increase in salinization of the upper soil layer was caused by the evaporative
382 concentration of salts at the soil surface. SAR values varied from 10-8 to 2-4
383 depending on the depth soil layer and its distribution was similar to the salinity



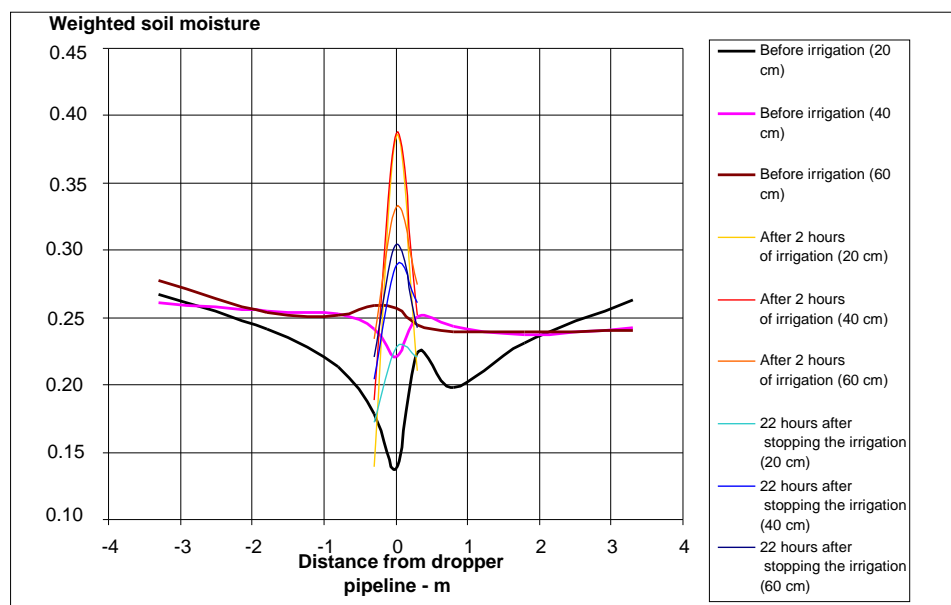
384 distribution. Active chalk values ranged from 15-20% to 30-33%, with higher
385 concentration at a depth of 20-60 cm, which did not change during the experiment.
386 Weighted soil moisture ranged from 0.14 to 0.36, which increased with depth.
387



388
389 Fig. 9. Soil salinity at different soil profile depths, measured at the first tensiometer
390 station.

391
392 During the study, the period averaged weighted soil moisture varied from 0.25 to 0.30,
393 with a dependency on distances from the dripper with an affected radius of up to 30
394 cm. Soil moisture increased with irrigation right away in the upper soil layer under the
395 dripper from 0.14 to 0.37 after 2 hours and 22 hours after irrigation stopped it
396 decreased to 23% (Fig. 10).

397
398



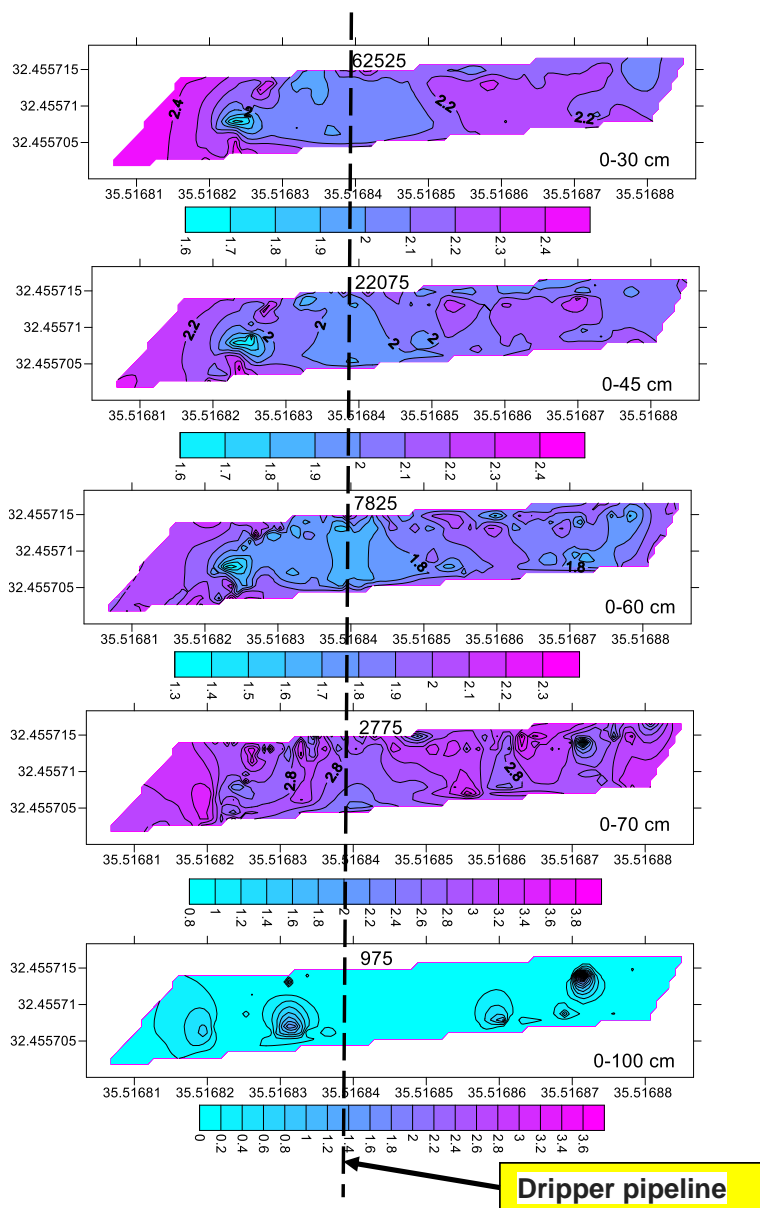
399

400 Fig. 10. Weighted soil moisture on different distances from dripper pipeline around
401 first tensiometer station

402

403 3.3. Soil salinity mapping using FDEM device

404 EC values obtained from FDEM measurements characterize the dissolved salts amount
405 and soil moisture. The maps show the salt flushing area progressing to a depth of 50-
406 60 cm (Fig.11). The salt flushing area width was about 0.5 m, demonstrating EC lower
407 than 2 dS/m, reaching EC values of 2.5 dS/m between rows. At a depth of 60-80 cm,
408 the soil salinity had a maximum of 2.5-3.0 dS/m. The travertine layer from a depth of
409 80 cm is probably dry, which does not enable ion movement that appears as very low
410 salinity values. This suggests that for matching EC values with laboratory results, the
411 FDEM strata should be in full saturation conditions (EC_{sat}). Otherwise, the correlation
412 between soil moisture and salinity is necessary. This relationship depends on the
413 lithological and chemical composition of the local soil profile. Figure 12 shows the
414 correlation between the ratio of laboratory EC measurements (EC_{sat}) to FDEM EC
415 measurements and weighted soil moisture according to soil characteristics of the study
416 site.

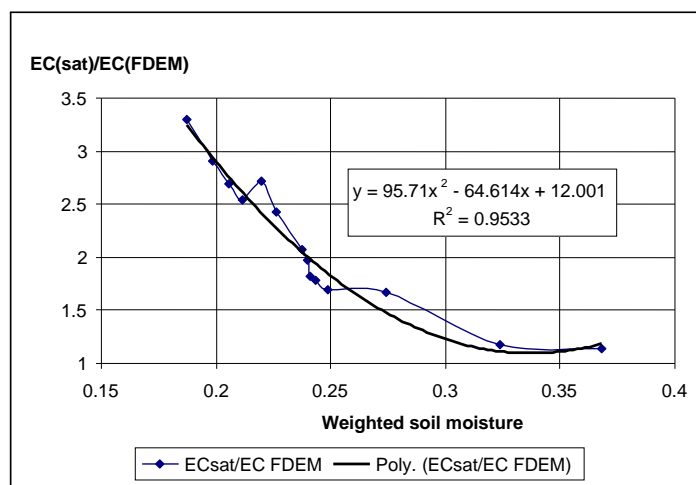


417

418

419 Fig. 11. FDEM EC values on the different depth of the soil profile.

420 Thus, under a weighted soil moisture content of 0.2, the EC values obtained using the
421 FDEM device (EC FDEM) will be approximately 3 times lower than those measured
422 in the soil saturation extract laboratory measurements (EC (sat)). Although, provided
423 the weighted soil moisture is greater than 0.32, EC measurements using FDEM would
424 be close to the laboratory soil test results.



425

426 Fig. 12. Correlation between the EC (sat) to EC FDEM ratio and the weighted soil
427 moisture at the Kibbutz Meirav mature olive plantation test site.

428

429 **3.4. Water and salt movement modeling for soil salinization prediction of** 430 **different irrigation water quality**

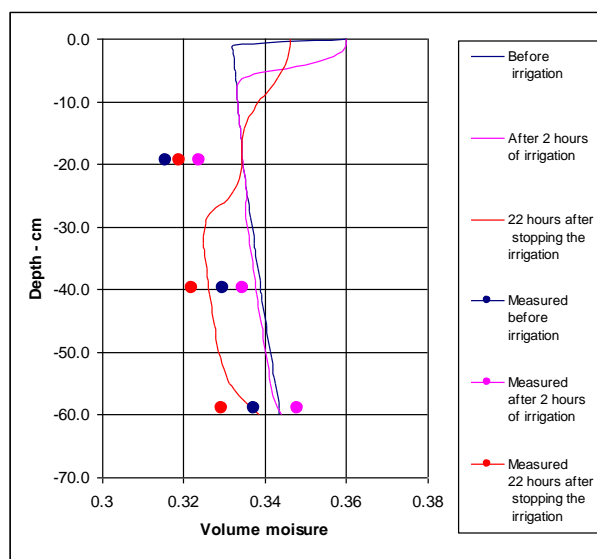
431

432 Fitting the model to the study site conditions was based on comparing the model
433 calculation results with measurements taken during the field experiment. The
434 comparison was made for soil volumetric moisture and soil salinity values in EC. The
435 best fit between model calculation and soil mechanical composition field
436 measurements was obtained for the silty clay type soil (Fig. 2). The volumetric
437 moisture model calibration was similar to the calculated results (Fig. 13). The
438 hydraulic conductivity of the soil saturated conditions according to the model was 0.02
439 cm per hour.

440 Differences between soil volumetric moisture measured in the field and calculated in
441 the model were: maximal -0.0187 (5.9% of the measured), minimal - 0.0029 (0.88%)
442 and on average - 0.0077 (2.39%). The soil salinity values calculated in the model were
443 similar to the salinity distribution obtained from the soil samples in the study site.
444 However, differences between soil salinity measured in the field and the one
445 calculated in the model ranged from 34% to 11% and on average - 28.8% (1.08
446 (dS/m)). This is because the soil salts movement model did not include the salts'



447 release and absorption processes in the soil. Soil suction, according to the calibrated
448 model calculations, decreased in the upper soil layer (up to 20 cm depth) immediately
449 after the irrigation began.
450

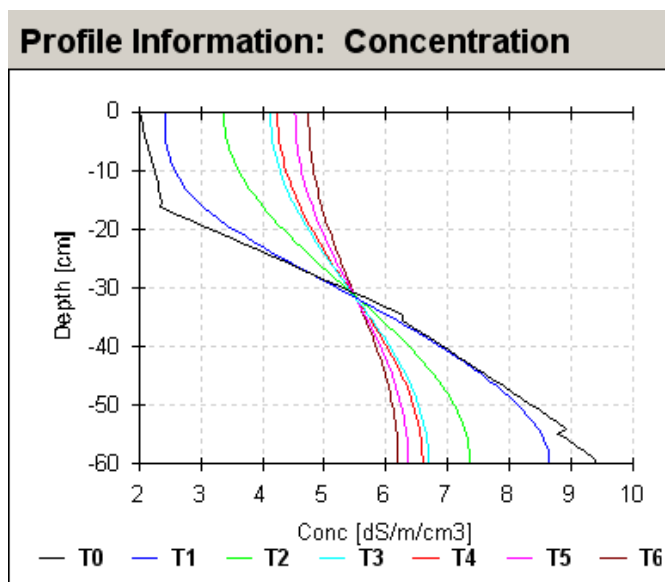


451

452 Fig. 13. Comparison of volumetric moisture values measured in a study section with
453 computerized values in the model. Model calibration results.

454

455 In deeper layers, it started after two hours, while 12 hours after irrigation ended soil
456 suction began to rise owing to soil drying. Changes in volume soil moisture were
457 consistent with changes in soil suction. Moisture increased immediately after irrigation
458 in the upper soil layer from 0.33 to 0.36 almost to a saturated state. After two hours
459 (end of irrigation) the moisture began decreasing. The results in the model show that in
460 the deep layers (below 30 cm from the soil surface) the moisture continued to decrease
461 probably due to a rather small amount of water and irrigation span. As a result of
462 irrigation by relatively saline water (3.13 dS/m), soil salinity (salts concentration)
463 increased in the upper soil layer (up to 30 cm depth) but decreased at the bottom of the
464 soil profile (Fig. 14). In both model and field measurements, the border between these
465 opposite salinity dynamics corresponded approximately to the root system depth, as
466 intensive development of trees appears in depth below 35 cm.

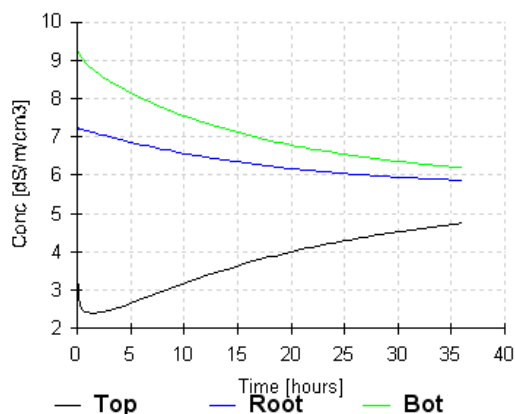


467

468 Fig. 14. Changes in soil salinity in the soil profile calculated in the model. Calibration
469 results of the model. T0 - start time (irrigation beginning); T1 - after two hours
470 (irrigation finish); T2 - after 12 hours; T3 - after 22 hours; T4 - after 24 hours; T5 -
471 after 30 hours; T6 - after 36 hours.

472

473 Fig. 15 shows the process of salts accumulating (or washing away) at the model's
474 outer boundaries. Near the soil surface at the TOP boundary, the salt concentration
475 initially decreased due to soil washing by irrigation, and after irrigation finished it
476 gradually increased over 36 hours, owing to evaporation from 2.5 dS/m to 4.7 dS/m.
477 At the root zone bottom (ROOT boundary), the salt concentration was constant, with a
478 small tendency to decrease. The salts concentration at the lower model boundary
479 (BOT) gradually decreased from 9.2 dS/m to 6.2 dS/m, which is probably related to
480 the horizontal movement of water together with dissolved salts from the dripper to the
481 travertine layer.



482

483

484 Fig. 15. Changes in salt concentration, calculated in the model at the upper model
485 boundary (TOP), at the root zone bottom (about 35 cm from the ground surface)
486 (ROOT) and the lower model boundary (BOT).

487

488 The soil salinity calibrated model simulates soil salinity patterns, with different water
489 quality irrigation between April to December. The data input to the model for
490 calculating the irrigation duration per day and daily evapotranspiration included the
491 olive plantation irrigation and daily evaporation and also evapotranspiration from the
492 Eden Farm meteorological station (Table 2).

493 Initial salt concentration values in the model soil profile (the 1st of April) were taken
494 from the field experiment soil sampling results. Soil profile and salts accumulation
495 predictions during the irrigation season show that under current water quality
496 conditions (3.13 dS/m) soil salinity may rise to 15-16 dS/m (Fig.16, A). The most
497 intense soil salinity change from 2.0 to 4.0 dS/m per month was in June, immediately
498 after irrigation increased. The model calculation results are consistent with soil salinity
499 monitoring during 2011 (fig.6). Irrigation by potable water (Fig.16, B) reduced soil
500 salinity to 7-9 dS/m.

501



502 Table 2. Irrigation and evaporation data used in the model

Month	Date	From start-day	From start-hour	Irrig. Dur.-hour	Irrig - mm	Irrig-mm/hour	Daily Evap-mm
April	0-10	10	240	7	2	0.286	2.00
	11-20	20	480	7	2	0.286	2.00
	21-30	30	720	10.6	3.02	0.285	3.02
May	1-10	40	960	12.9	3.69	0.286	3.69
	11-20	50	1200	12.9	3.69	0.286	3.69
	21-31	61	1464	17.6	5.01	0.285	5.01
June	1-10	71	1704	13.5	3.85	0.285	3.85
	11-20	81	1944	13.5	3.85	0.285	3.85
	21-30	91	2184	13.8	3.93	0.285	3.93
July	1-10	101	2424	13.8	3.93	0.285	3.93
	11-20	111	2664	13.8	3.93	0.285	3.93
	21-31	122	2928	12.8	3.66	0.286	3.66
August	1-10	132	3168	14.1	4.02	0.285	4.02
	11-20	142	3408	16.7	4.75	0.284	4.75
	21-31	153	3672	13.9	3.97	0.286	3.97
September	1-10	163	3912	13.9	3.97	0.286	3.97
	11-20	173	4152	13.9	3.97	0.286	3.97
	21-30	183	4392	10.1	2.88	0.285	2.88
October	1-10	193	4632	9.3	2.66	0.286	2.66
	11-20	203	4872	9.3	2.66	0.286	2.66
	21-31	214	5136	4	1.15	0.286	1.15
November	1-10	224	5376	3.6	1.02	0.283	1.02
	11-20	234	5616	3.6	1.02	0.283	1.02
	21-30	244	5856	1.2	0.34	0.283	0.34

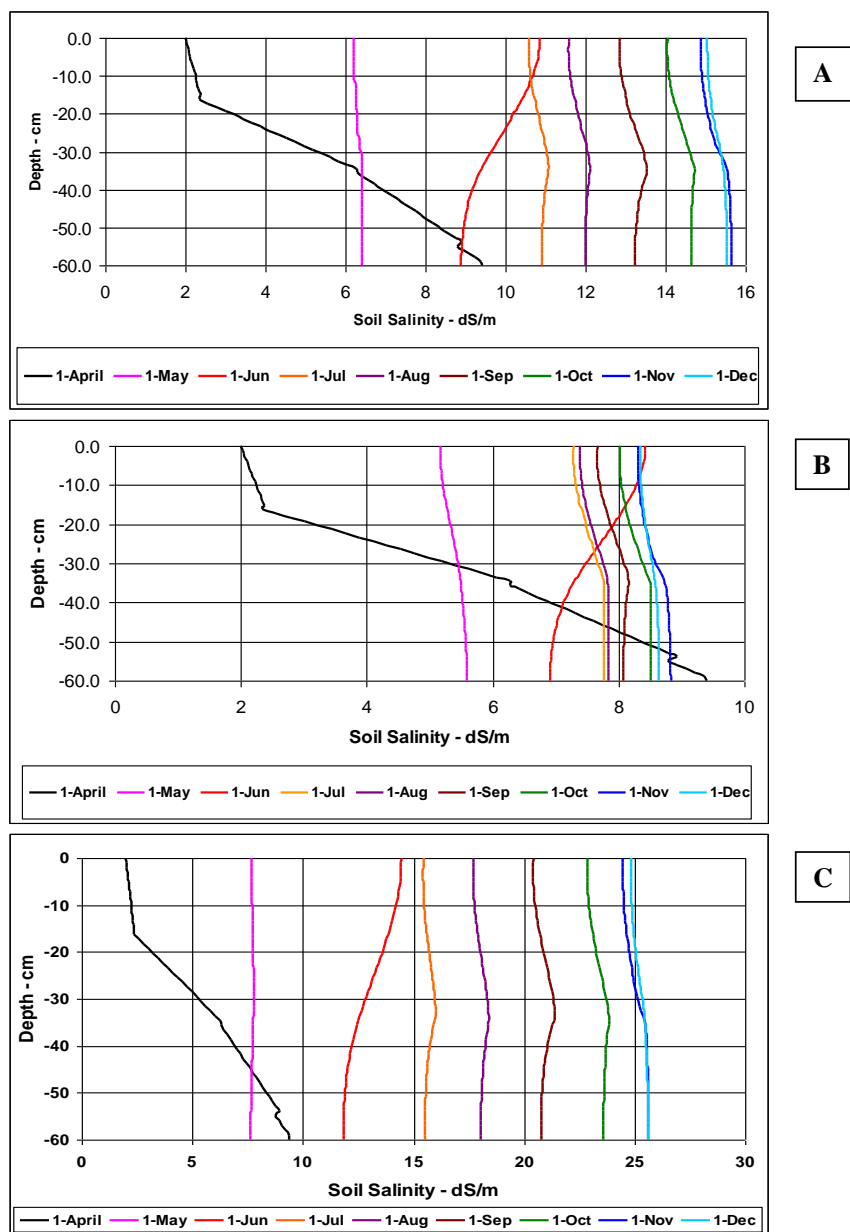
503

504

505 Irrigation by brackish water during the summer months (Fig. 4, C) caused substantial
 506 increases in soil salinity, reaching a very high EC value of about 24-26 dS/m.

507 Irrigating with such water during summer months, might increase EC in 2 - 3 dS / m
 508 per month on average, owing to salt accumulation in the soil profile. Brackish water
 509 irrigation (EC> 5 dS/m), might cause the entire soil profile turning saline to the point
 510 that could harm the trees.

511



512

513 Fig. 16. Salts accumulation predictions in the soil during irrigation season under
514 different water salinity: A - 3.13 dS/m (available today); B - 1.5 dS/m (potable water);
515 C - 5.5 dS/m (brackish water).



516

517 4. Conclusions

518

519 The combined use of various research methods, including soil salinity monitoring,
520 field experiments, remote sensing (FDEM) and water and salts movement modeling in
521 the unsaturated soil profile allowed assessment of salinization processes of chalky soil
522 in an irrigated olive plantation in the Beit She'an Valley. Under the existing drip
523 irrigation regime, water with a dissolved salt content of 3.13 dS/m, and the presence of
524 an impermeable travertine layer close to the soil surface, the salinization process is
525 characterized by a tendency for salts to accumulate in the upper root zone of the trees
526 after the summer irrigation season. During irrigation, the soluble salts are rapidly
527 leached to the depth and sides of the dripper in the upper 20-30 cm soil layer.
528 However, after a short time within 24 hours after the completion of the irrigation
529 cycle, the level of salinity in the soil begins to increase again. Soil dries out and salt
530 accumulates near the surface due to evapotranspiration.

531

532 The FDEM device made it possible to study the spatial distribution and concentration
533 of the dissolved salts, taking into account the existing weight moisture distribution in
534 the soil at the time of measurement. The FDEM EC maps show the salt flushing area
535 development at a depth of 50-60 cm. The width of the salt flushing area was ~0.5 m.
536 By combining the soil salinity and moisture field sampling results and measuring soil
537 salinity by FDEM, a correlation between the EC soil measurements in the laboratory
538 by the traditional method and those measured by FDEM for a given soil type was
539 obtained. The established relationship will allow for a reasonable comparison of soil
540 salinity measurement results obtained by different methods, as soil salinity mapping
541 accuracy by FDEM is higher and its cost lower.

542

543 The one-dimensional model created for water and movement of dissolved salts showed
544 the danger of using brackish water for irrigation. Since soil salinization exceeds an
545 acceptable level for trees, the use of potable water for irrigation, if possible, will help
546 to reduce soil salinization.



547 To enable a tailor-made irrigation scheme, a database of the topics reviewed in this
548 paper should be established. The database should include information on the changes
549 in physical and chemical parameters affecting soil salting processes that will enable
550 contemporary mapping and salinity forecasting and hydrochemical factors of various
551 soil and irrigation conditions in the region.

552

553 **5. Code and data availability**

554 Data and code are available in the supplement

555

556 **6. Author contribution**

557

558 Vladimir Mirlas designed and carried out the field experiments, performed the Hydrus
559 simulations. Naftaly Goldshleger designed and carried out the field experiments,
560 performed measurements and mapping of the soil electrical conductivity using an
561 FDEM device. Asher Aizenkod did the irrigation data processing and Yaakov Anker
562 analyzed the results and prepared the manuscript with contributions from all co-
563 authors.

564 **7. Acknowledgments**

565

566 This article is based on the results of scientific research carried out as project 855-
567 0066-12 “Identification and assessment of soil salinization risk as a result of
568 agricultural activity in the Beit She'an Valley” by a team of researchers and technical
569 personnel of the Soil Erosion Research Station of the Ministry of Agriculture and
570 Rural Development (MOAG), Israel: Dr. V. Mirlas (main researcher), Dr. N.
571 Goldshleger (researcher), A. Aizenkod (researcher, field survey center, MOAG), R.
572 Ben-Binyamin (technician), Y. Barnay-Betsalel (technician), and I. Sapogineth
573 (technician, the eastern R&D center, Ariel University).

574 The research was funded by the Keren Kayemeth LeIsrael - Jewish National Fund



575 (KKL – JNF) and supported by the Ministry of Agriculture and Rural Development of
576 Israel. The authors particularly thank the technical team of the SERS and the Eastern
577 R&D center, Ariel University: R. Ben-Binyamin, Y. Barnay-Betsalel, M. Gottesman,
578 E. Fizik and I. Sapogineth for their assistance in the field investigations.

579

580 8. Reference

- 581 Abu Awward, A., M.: Influence of different water quantities and qualities on
582 lemon trees and soil salt distribution at the Jordan Valley, *J. Agricultural Water*
583 *Management*, 52 (1), 53-71, 2001.
- 584 Bear, J.: *Dynamics of Fluid in Porous Media*, Elsevier, New York, NY, 1972.
- 585 Ben Dor, Y., Metternicht, G., Goldshleger, N., Mor, E., Mirlas, V., Basson, U.:
586 Review of remote sensing-based methods to assess soil salinity, In: *Remote*
587 *sensing of soil salinization, Impact on land management*, (eds. G. Metternicht, J.A.
588 Zinck), pp. 39-63, CRC Press, Taylor & Francis Group, LLC, New York, USA.
589 DOI:10.1201/9781420065039.ch3, 2009a.
- 590 Ben Dor, Y., Goldshleger, N., Mor, E., Mirlas, V., Basson, U.: Combined active
591 and passive remote sensing methods for assessing soil salinity: a case study from
592 Jezre'el Valley, Northern Israel, In: *Remote sensing of soil salinization, Impact on*
593 *land management*, (eds. G. Metternicht, J.A. Zinck), pp. 236-253, CRC Press,
594 Taylor & Francis Group, LLC, New York, USA. DOI:10.1201/9781420065039-
595 .ch12, 2009b.
- 596 Benyamini, Y., Marish S., Mirlas V., Gotesman M.: Soil Salinization and
597 Rehabilitation, In: *Proc., The Ann. Meeting, Israel Geog. Soc., Tel-Aviv, Israel*,
598 128 -129, 1998.
- 599 Benyamini, Y., Marish S., Mirlas V., Gotesman M.: Impact of Subsurface Drainage
600 on Groundwater Regime in Irrigated Fields in Israel. In: *Proc. Inter. Conf. "Water*
601 *and Environment: Resolving Conflicts in the Development of Dry Lands"*, Beer-
602 Sheba, Israel, 4-7 June. The Center for Water Science and Technology (CWST),
603 Ben-Gurion University of the Negev, 56-57, 2000.
- 604 Benyamini, Y., Mirlas V., Marish S., Gotesman M., Fizik, E., and Agassi, M.: A
605 survey of soil salinity and groundwater level control systems in irrigated fields in
606 the Jezre'el Valley, Israel, *J. Agricultural Water Management*, 76(3), 181-194,
607 2005.
- 608 Bhardwaj, A. K., Mandal, U.K., Bar-Tal, A., Gilboa, A., and Levy, G. J.:
609 Replacing saline-sodic irrigation water with treated wastewater: effects on



- 610 saturated hydraulic conductivity, slaking and swelling, *J. Irrigation Science*, 26 (2),
611 139-146, 2008.
- 612 Boone, A., Samuelsson, P., Gollvik, S., Napoly, A., Jarlan, L., Brun, E.,
613 Decharme, B.: The interactions between soil-biosphere-atmosphere land surface
614 model with a multi-energy balance (ISBA-MEB) option in SURFEXv8-Part 1:
615 Model description, *Geosci. Model Dev.* 10, 843–872, 2017.
- 616 Gafni, A., Salinger, Y.: Hydraulic and salinity regime of two affected sites in the
617 Jezre’el Valley, Israel, *J. Hydrol. Proc.* 6, 55–65, 1992.
- 618 Celia, M.A., Bououtas, E.T., Zarba, R.L.: A general mass-conservative numerical
619 solution for the unsaturated flow equation, *Water Resour. Res.*, 26, 1483-1496,
620 1990.
- 621 Corwin, D.L. and Lesch, S.M.: Apparent soil electrical conductivity measurements
622 in agriculture, *Computer Electronics in Agriculture*46: 11–43, 2005.
- 623 Crank, J. and Nicolson, P.: A practical method for numerical evaluation of
624 solutions of partial differential equations of the heat-conduction type, *Proc.*
625 *Cambridge Philos. Soc.*, 43 pp. 50–67, 1947.
- 626 Farifteh, J., van der Meer, F., Atzberger, C., and Carranza, E.J.M.: Quantitative
627 analysis of salt-affected soil reflectance spectra: A comparison of two adaptive
628 methods (PLSR and ANN), *Remote Sensing of Environment*, 110: 59–78, 2007.
- 629 Feddes, R., Hoff, H., Bruen, M., Dawson, T., de Rosnay, P., Dirmeyer, P.,
630 Jackson, R.B., Kabat, P., Kleidon, A., Lilly, A. and Pitman A.J.: Modeling root
631 water uptake in hydrological and climate models, *Bull. Amer. Meteor. Soc.*, 82,
632 2797–2809doi:10.1175/15200477(2001)082%3C2797%3AMRWUIH%3-
633 E2.3.CO%3B2, 2001.
- 634 Fletcher, C.: *Computational Galerkin Methods*, Springer-Verlag New York Inc,
635 303 pp. DOI: 10.1007/978-3-642-85949-6, 1983.
- 636 Garrigues, S., Olliso, A., Carrer, D., Decharme, B., Calvet, J.C., Martin, E.,
637 Moulin, S., Marloie, O.: Impact of climate, vegetation, soil and crop management
638 variables on multi-year ISBA-A-gs simulations of evapotranspiration over a
639 Mediterranean crop site, *Geosci. Model Dev.* 8, 3033–3053, 2015.
- 640 Guimberteau, M., Zhu, D., Maignan, F., Huang, Y., Yue, C., Dantec-N d lec, S.,
641 Ottl, C., Jornet-Puig, A., Bastos, A., Laurent, P., Goll, D., Bowring, S., Chang, J.,
642 Guenet, B., Tifafi, M., Peng, S., Krinner, G., Ducharme, A. s., Wang, F., Wang, T.,
643 Wang, X., Wang, Y., Yin, Z., Lauerwald, R., Joetzjer, E., Qiu, C., Kim, H., Ciais,
644 P.: ORCHIDEE-MICT (v8.4.1), a land surface model for the high latitudes: model
645 description and validation, *Geosci. Model Dev.* 11, 121–163, 2018.



- 646 Kool, J.B., Parker, J.C., van-Genuchten, M. Th.: Determining soil hydraulic
647 properties from one-step outflow experiments by parameter estimation: I. Theory
648 and numerical studies, *Soil Sci. Soc.Am. J.*, 49,1348-1354, 1985.
- 649 Kruseman, G.P., De Ridder, N.A.: Analysis and Evaluation of Pumping Test Data,
650 International Institute for Land Reclamation and Improvement/ ILRI, Wageningen,
651 The Netherlands, 18–20 pp., 1976.
- 652 Leij, F.G., Skaggs, T.H., van-Genuchten,M.Th.: Analytical solutions for solute
653 transport in three-dimensional semi-infinite porous media, *Water Resour.Res.*,
654 27(10), 2719-2733, 1991.
- 655 Mandal, U.K., Bhardwaj, A.K., Warrington, D.N., Goldstein, D., Bar-Tal, A.,
656 Levy, G.J.: Changes in soil hydraulic conductivity, runoff, and soil loss due to
657 irrigation with different types of saline-sodic water, *J. Geoderma*, 144(3-4), 509-
658 516, 2008(a).
- 659 Mandal, U.K., Warrington, D.N., Bhardwaj, A.K., Bar-Tal, A., Kautsky, L., Minz,
660 D., and Levy, G.J.: Evaluating impact if irrigation water quality on a calcareous
661 clay soil using principal component analysis, *Geoderma*, 144(1-2), 189-197,
662 2008(b).
- 663 Mirlas, V., Benyamini, Y., Marish, S., Gotesman, M., Fizik, E., Agassi, M.:
664 Method for Normalization of Soil Salinity Data, *J. of Irrigation and Drainage*
665 *Engineering*, 129(1), 64-66, 2003.
- 666 Mirlas, V., Benyamini, Y., Gotesman, M., Fizik, E., and Agassi, M.: Long-term
667 changes in groundwater regime of a semi-confined aquifer in Jezre'el Valley,
668 Israel, *J. World Assoc.Soil Water Conserv.*, J1: 98-112, 2006.
- 669 Mirlas, V., Benyamini, Y.,Miron, M., Peres, M., Yasur, E.: Development of
670 groundwater flow and salt transport models for the non-saturation zone of the soil
671 in the Hula Valley, Annual meeting of the Israel Geography Society, 1-3.01.2006,
672 Jerusalem, Israel, 63-64 (in Hebrew), 2006.
- 673 Mirlas, V.: Assessing soil salinity hazard in cultivated areas using MODFLOW
674 model and GIS tools: A case study from the Jezre'el Valley, Israel, *J. Agriculture*
675 *Water Management*. Vol. 109, 144-154, 2012.
- 676 Mohammad, M., J., Mazahreh, N.: Changes in soil fertility parameters to irrigation
677 of forage crops with secondary treated wastewater, *J. Communication in Soil*
678 *Science and Plant Analysis*, 34(9 & 10), 1281-1294, 2003.
- 679 Pandit, R., Parrotta, J.A., Chaudhary, A.K., Karlen, D.L., Luis, D., Vieira, M.,
680 Anker, Y., Chen, R., Morris, J., Ntshotsho, P., Pandit, R., Parrotta, J.A.,
681 Chaudhary, A.K., Douglas, L., Luis, D., Vieira, M., Anker, Y., Chen, R., Morris,
682 J., Harris, J.: A framework to evaluate land degradation and restoration responses
683 for improved planning, *Ecosyst. and People* 15, 1–18, 2020.



- 684 Rui Manuel Almeida Machado,R., Serralheiro, R.: Soil Salinity: Effect on
685 Vegetable Crop Growth, Management Practices to Prevent and Mitigate Soil
686 Salinization. Horticulturae 2017, 3, 30.13 pp. doi:10.3390/horticulturae3020030,
687 2017.
- 688 Simunek, J.,and van-Genuchten, M. Th.: Numerical model for simulating multiple
689 solute transport in variably-saturated soil, Proc. "Water Pollution III: Modeling,
690 Measurement, and Prediction". Ed. L.C. Wrobel and P. Latinopoulos, Computation
691 Mechanics Publ,Ashurst Lodge, Ashjur, Southampton, UK, pp. 21-30, 1995.
- 692 Simunek, J., Sejna, M., van Genuchten, M.Th.: The HYDRUS-1D software
693 package for simulating the one-dimensional movement for water, heat,and multiple
694 solutes in variably-saturated media, version 2.0, IGWMC-TPS 70. U.S. Salinity
695 laboratory, Agricultural Research Service, U.S. Department of Agriculture,
696 Riverside, California, 1998.
- 697 Toride, N., Leij, F.J., van Genuchten, M.Th.: A comprehensive set of analytical
698 solution for no equilibrium solute transport with first-order decay and zero-order
699 production, Water Resour.Res., 29(7), 2167-2182, 1993.
- 700 van Genuchten M. Th.: A Closed-form Equation for Predicting the Hydraulic
701 Conductivity of Unsaturated Soils, J. Soil Science Society of America
702 <https://doi.org/10.2136/sssaj1980.03615995004400050002x>, 1980.
- 703 van Genuchten, M.Th.: A numerical model for water and solute movement in and
704 below the root zone, Research Report No 121, U.S. Salinity laboratory , USDA,
705 ARS, Riverside, California, 1987.
- 706 van Genuchten, M. Th., and Wagenet, R.J.: Two-site/two region models for
707 pesticide transport and degradation: Theoretical development and analytical
708 solutions, Soil Sci. Soc.Am. J., 53, 1303-1310, 1989.
- 709 Wada, Y., Flörke, M., Hanasaki, N., Eisner, S., Fischer, G., Tramberend, S., Satoh,
710 Y., Van Vliet, M.T.H., Yillia, P., Ringler, C., Burek, P., Wiberg, D.: Modeling
711 global water use for the 21st century: The Water Futures and Solutions (WFaS)
712 initiative and its approaches, Geosci. Model Dev. 9, 175–222, 2016.
- 713